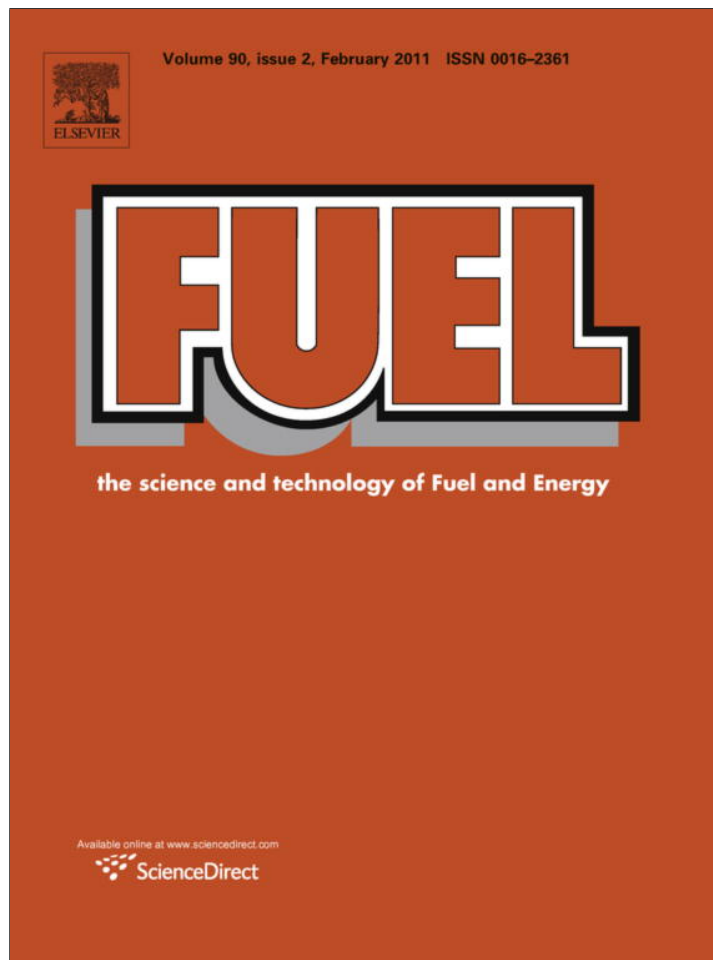


Provided for non-commercial research and education use.
Not for reproduction, distribution or commercial use.



This article appeared in a journal published by Elsevier. The attached copy is furnished to the author for internal non-commercial research and education use, including for instruction at the authors institution and sharing with colleagues.

Other uses, including reproduction and distribution, or selling or licensing copies, or posting to personal, institutional or third party websites are prohibited.

In most cases authors are permitted to post their version of the article (e.g. in Word or Tex form) to their personal website or institutional repository. Authors requiring further information regarding Elsevier's archiving and manuscript policies are encouraged to visit:

<http://www.elsevier.com/copyright>



Prediction of product quality for catalytic hydrocracking of vacuum gas oil

Haitham M.S. Lababidi^{a,*}, Dduha Chedadeh^b, M.R. Riazi^a, Ayman Al-Qattan^b, Hamad A. Al-Adwani^a

^a Chemical Engineering Department, College of Engineering & Petroleum, Kuwait University, P.O. Box 5969, Safat 13060, Kuwait

^b Kuwait Institute for Scientific Research, P.O. Box 24885, Safat 13109, Kuwait

ARTICLE INFO

Article history:

Received 22 January 2010

Received in revised form 27 August 2010

Accepted 22 September 2010

Available online 20 October 2010

Keywords:

Hydrocracking

Vacuum gas oil

Product distribution

Predictive model

Soft sensor

ABSTRACT

The main objective of this work is to develop a predictive model for predicting the product quality of vacuum gas oil (VGO) hydrocracking process. Experimental data were obtained using a pilot plant hydrocracking catalytic reactor loaded with the same catalyst type used in a local refinery. Two sets of experimental runs were conducted under various operating conditions. The first one consisted of 18 runs and was used for parameter estimation, while the second set consisted of 29 runs and was used for model validation. Distillation curves of the cracked products were obtained using the simulated distillation (SimDist) test. A distribution model based on probability density function was used to develop the predictive model. The distribution model presents the boiling point as a function of the distilled weight fraction. Model parameters were estimated and related to the specific gravity of the cracked product. Model validation results showed that the proposed model is capable of predicting the distillation curves of the hydrocracked products accurately, especially at high operating severity. Simplicity and accuracy of the developed model makes it suitable for online analysis, to estimate the conversion as well as the product distribution of hydrocracking units in refineries.

© 2010 Elsevier Ltd. All rights reserved.

1. Introduction

The purpose of hydrocracking process in petroleum refineries is to convert heavy oil and heavy residues into more useful light and high quality products such as naphtha, gasoline, jet fuel and diesel fuel. With decreasing resources of light and medium crude oils, cracking processes are vital to benefit from the bottom of the barrel, heavy oils (API < 20), tar sands and shale oils. Furthermore, cracking of heavier fractions is essential to satisfy the demand of feedstock to the expanding petrochemical industries.

Hydrocracking is defined as the transformation of large (high boiling point) hydrocarbon molecules into smaller (low boiling point) molecules in the presence of hydrogen. This transformation occurs due to the breaking of carbon–carbon bonds or the removal of heteroatoms that is bonding to two unconnected pieces of hydrocarbons. Before the carbon bonds can be broken and the large molecules cracked, it is often necessary to hydrogenate the molecules and to saturate the aromatic rings that contain most of carbon atoms [1]. The main advantage of hydrocracking over catalytic cracking is the production of more hydrogenated and high quality products. Furthermore, in hydrocracking processes there is no carbon rejection (loss of carbon from feedstock) whereas in catalytic cracking certain amount of carbon is lost as carbon deposit on the catalyst [2].

Hydrocracking (HCR) processes are commonly used in refineries for converting vacuum gas-oil (VGO) into higher-valued and lighter transportation fuels, namely, naphtha, aviation turbine kerosene (ATK), and diesel. Such processes are important for modern refineries, where hydrotreating units are upgraded to hydrocracking units [3–5].

Hydrocracked products from the HCR units are separated into different fractions, which constitute the blending stocks of the final products. The quality of the products varies widely with operating conditions, whereas the cracking yield is reduced with time due to catalyst deactivation. For these reasons, continuous monitoring of the products is very important to avoid off spec petroleum fractions, which usually cause problems downstream at the blending stage. However, laboratory analysis of product samples is time consuming and may be insufficient to track variations in product quality. For such applications, soft sensors are desirable for on-line analysis, and can be implemented to obtain the product quality, such as composition or cracking conversion, using conventional on-line measurements of process conditions.

Soft sensors consist mainly of predictive models that describe the relationship between the predicted variables and the measured variables. They can be distinguished into two different classes, namely model-driven and data-driven [6]. Model-driven soft sensors are based on first principle mathematical models which describe the physical and chemical background of the process [7,8]. They are primarily developed for off-line planning and optimization purposes with low sampling rates, because they usually require intensive computation. On the other hand, data-driven

* Corresponding author. Tel.: +965 4985778.

E-mail address: haitham.lababidi@ku.edu.kw (H.M.S. Lababidi).

predictive models are based on actual data measured within the operational plants, and thus describe the real process conditions. They are suitable for monitoring process output quality at high sampling rates, and thus essential for process control applications. The most popular techniques applied to data-driven models are regression, Artificial Neural Networks [9] and Neuro-Fuzzy Systems [10].

The main objective of this work is to develop a predictive model for predicting the product quality of VGO hydrocracking process. Section 2 describes the experimental setup and procedure used in obtaining the operational data, which consists mainly of the temperature distribution curves for the cracked products at different operating conditions. The third section presents the development of the proposed prediction model, followed by validation of model predictions against experimental data.

2. Experimental

Experimental data used in the current study was generated using a pilot HCR plant. A schematic diagram of the pilot plant configuration is shown in Fig. 1. It consists of a once-through (no recycle) microreactor followed by high and low pressure separators. The reactor is a flange type, with a total volume of 505 ml and an internal diameter of 2.8 cm. It was loaded with 128 ml of catalyst diluted with 136 ml of carborundum. Coarse carborundum and inert alumina balls were placed above and below the catalyst bed as pre- and post-heating zones.

Heated feed and hydrogen are introduced to the reactor in a down co-current flow mode. The reactor consists of five reaction zones, each equipped with a built-in furnace which is independently controlled to provide the required heating. Each reaction zone is equipped with a K-Type thermocouple to measure and control the reactor bed temperature.

Vacuum gas oil (VGO) feedstock and the HCR catalyst used in the runs were supplied by a local refinery. HCR reaction severity was varied by operating at different bed temperatures (T_{bed}) and throughputs, i.e. Liquid Hourly Space Velocity (LHSV). Three bed

temperatures (370, 380 and 390 °C) and three LHSVs (1.0, 1.5 and 2.0 h^{-1}) were selected.

After loading the reactor with the catalyst, presulfiding was carried out to achieve the desired hydrocracking activity. This was followed by operating the reactor at fixed conditions (LHSV = 1.5 h^{-1} and T_{bed} = 380 °C) until reaching stable hydrocracking conversion. During this stabilization period, product samples were collected and analyzed. Catalyst stabilization was mainly monitored using the density of the product, and confirmed via distillation analysis.

The hydrocracking experimental runs proceeded by adjusting the desired bed temperatures and space velocities (LHSVs). Product samples were collected for laboratory analysis at specific intervals throughout the runs according to planned experimental schedules (Fig. 2). One product oil sample and one off-gas sample were collected and analyzed for each operating condition.

Two experimental runs were considered in this work, Run-1 and Run-2. The same VGO feedstock, catalyst type and operating conditions were used for both runs. Furthermore, fresh catalyst was loaded for each experimental run. The main difference between the two runs is that for Run-2 the catalyst bed is kept on stream for longer period before starting the experimental schedule and sampling. The experimental schedules of both runs were planned to cover the combinations of the three bed temperatures (370, 380 and 390 °C) and three LHSVs (1.0, 1.5 and 2.0 h^{-1}). The schedule for Run-1 is shown in Fig. 2. It consists of 18 tests and repeats every combination twice. The schedule of Run-2 followed similar experimental plan, but consisted of 29 tests because the combinations were repeated more than twice.

2.1. Sample analysis

Laboratory analyses mainly included density and simulated distillation (SimDist) for the liquid product samples, and refinery gas analyzer (RGA) gas analysis for samples from the vented off-gases. The ASTM D5002 standard test method was used to measure the density of the collected samples using a digital density analyzer

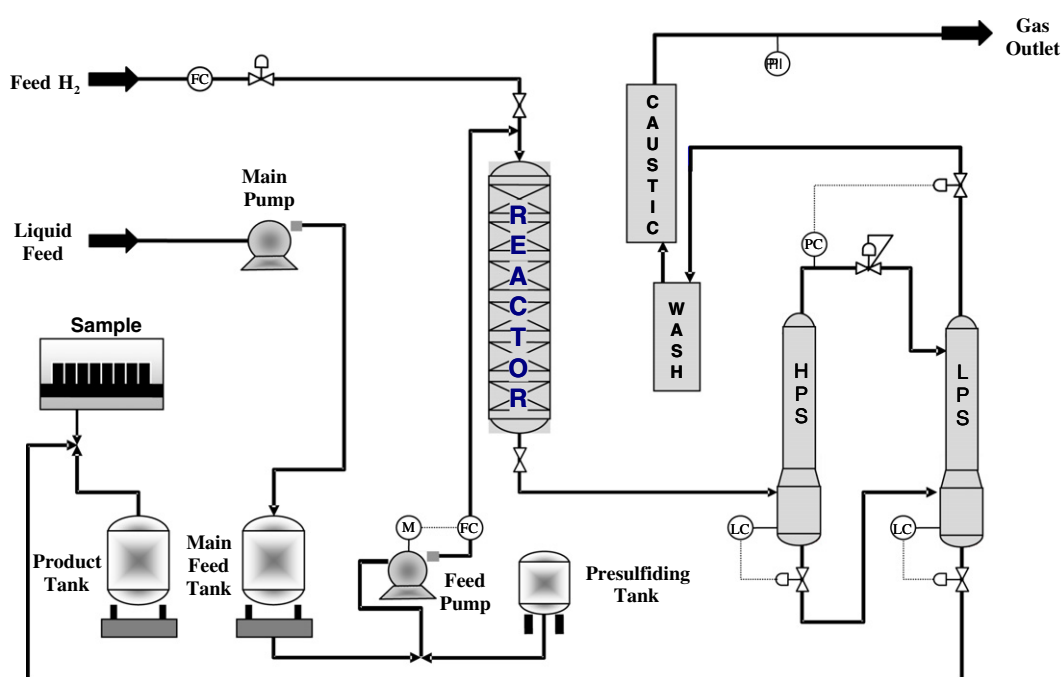


Fig. 1. Schematic of the pilot plant used for the experimental runs.

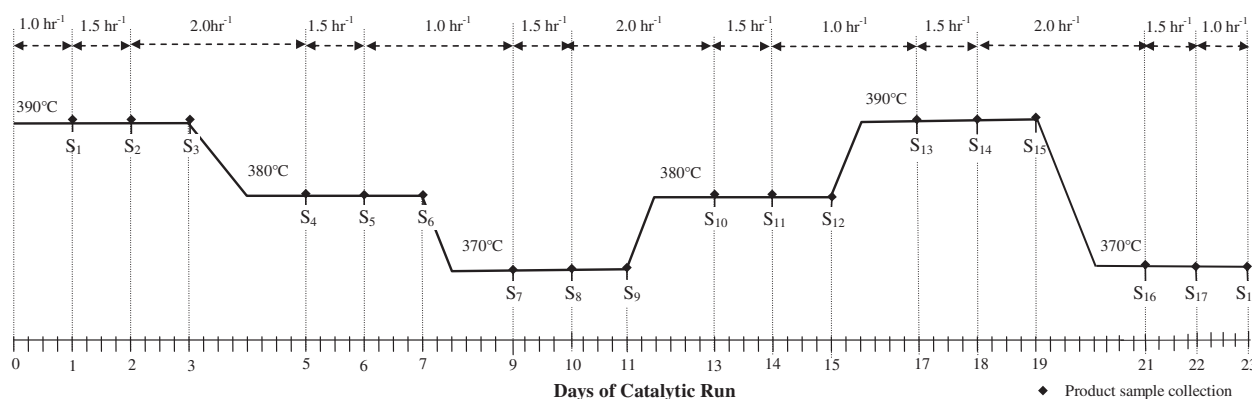


Fig. 2. Schedule of hydrocracking experiment, Run-1.

based on oscillation frequency. For the range of measured densities, the repeatability of the measurements is 0.00078.

SimDist ASTM D2887 standard method was used to determine the boiling range distribution of the VGO feed and cracked product. SimDist is a gas chromatography (GC) technique used to characterize petroleum fractions and products. This analytical tool permits quick determination of the boiling range distribution of petroleum fractions and is widely used to replace the time-consuming conventional distillation methods D86 or D1160. For SimDist method, the repeatability of the measurements ranges from 0.8 °C for 10% and 1.2 °C for 95% fractions.

Analysis of the off-gases is important for adjusting the material balance. Gas samples were collected in gas cylinders and tested in a refinery gas analyzer (RGA), which is a GC analyzer for gas analysis suitable for most types of refinery gases. Errors resulted from closing the material balances ranged from 0.2% to 5.4%.

2.2. Experimental data

Specific gravity (density at 15 °C) measurements for all product samples collected for Run-1 (S1–S18) and Run-2 (SC1–SC29) are listed in Table 1. Repeatability of specific gravity results for tests at same operating conditions is clearly illustrated in Figs. 3 and 4. The plots in both figures consider the sequence at which the samples were collected. For instance, sample S17 was collected (12 days) after S8. Furthermore, all Run-2 samples were collected after operating the reactor for more than 30 days. The results show clearly that samples collected for the same conditions become slightly heavier (higher specific gravity) with time. This is mainly due to catalyst deactivation. As the catalyst is kept on stream its activity declines and less cracking is achieved. The main conclusion is that the samples collected from different tests are not the same, even for those repeated at the same conditions.

It is also clear from the plots in Figs. 3 and 4 that increasing the operational severity results in lighter (lower specific gravity) products. This is due to the fact that as temperature increases and/or space velocity decreases (increasing residence time) the rate of hydrocracking increases, hence, the density decreases indicating better quality product.

Effect of reaction temperature on the boiling point curves of the cracked products for space velocity $LHSV = 2.0 \text{ h}^{-1}$ is shown in Fig. 5. Whereas effect of space velocity is shown in Fig. 6 for $T_{\text{bed}} = 390 \text{ °C}$. The boiling point plots indicate clearly that increasing the reaction severity (increasing temperature and decreasing space velocity) increases the amount of cracking, hence, the yield of lighter fractions. In addition, the plots show clearly the discrepancies in the boiling point curves for the experimental runs that were carried out at the same conditions. Dotted curves are below

the solid ones for all plots. This means that runs carried out at later time experienced less cracking. As mentioned above, this is mainly due to catalyst deactivation.

Another parameter, which is important to quantify the amount of cracking achieved, is conversion. Conversion can be defined as the percentage of the 288 °C + fraction of the feed cracked to lighter fractions:

$$\text{Conversion} = \frac{C_{F,288+} - C_{P,288+}}{C_{F,288+}} \quad (1)$$

where, $C_{F,288+}$ = 288 °C + fraction of the feedstock (wt.%), $C_{P,288+}$ = 288 °C + fraction of the cracked product (wt.%).

Using the boiling point curve, $C_{F,288+}$ and $C_{P,288+}$ are simply calculated as the intersections of the $T = 288 \text{ °C}$ line (shown in Figs. 5 and 6 as vertical dotted line) with the boiling point curves of the feed and product, respectively.

The relationship between the product density and conversion is shown in Fig. 7. The plot shows clearly that the density of the products decreases (lighter products) as conversion increases.

3. Predictive model

There are a number of distribution models available in the literature that are applied to petroleum mixtures [11–13]. The Gamma distribution model was originally proposed for gas condensate mixtures [11]. The distribution model proposed by Riazi [12,14] was specifically developed for heavy oil and heavy residues and petroleum products. This model can be used to estimate various properties such as distillation data, molar distribution, density and molar refraction distribution.

Distillation data (boiling point curve such as ASTM D2887) and density or specific gravity of petroleum mixtures are the most important physical properties of petroleum mixtures, for the design and operation of various refining units. Using available thermodynamic methods, majority of the physical and thermodynamic properties can be derived. Distillation data is also vital in determining the quality and specification of petroleum products [14].

The cracking conversion prediction model proposed in this work is based on the distribution model originally developed by Riazi [12,13], for estimating the properties of C_{7+} fractions from distillation data as presented in the ASTM Manual 50 [14]. The probability density function is described mathematically for the boiling point distribution in the following form:

$$\frac{T - T_0}{T_0} = \left[\frac{A}{B} \ln \left(\frac{1}{1-x} \right) \right]^{1/B} \quad (2)$$

where T is the boiling temperature from the distillation curve in degrees Kelvin and x is the corresponding cumulative volume or

Table 1
Specific gravity results for the product samples of the experimental runs.

Run-1				Run-2			
Sample	Temp.(°C)	LHSV (hr ⁻¹)	Density @ 15 °C	Sample	Temp. °C	LHSV (hr ⁻¹)	Density @ 15 °C
S1	390	1	0.7169	SC1	380	1.5	0.7555
S2		1.5	0.7127	SC2		2	0.7777
S3		2	0.7236	SC3	370	2	0.7949
S4	380	2	0.7532	SC4		1.5	0.7923
S5		1.5	0.7393	SC5		1	0.7711
S6		1	0.7211	SC6	380	1	0.7346
S7	370	1	0.7480	SC7		1.5	0.7505
S8		1.5	0.7659	SC8		2	0.7672
S9		2	0.7845	SC9	390	2	0.7505
S10	380	2	0.7641	SC10		1.5	0.7348
S11		1.5	0.7488	SC11		1	0.7217
S12		1	0.7281	SC12	380	1	0.7524
S13	390	1	0.7167	SC13		1.5	0.7540
S14		1.5	0.7269	SC14		2	0.7708
S15		2	0.7431	SC15	370	2	0.7967
S16	370	2	0.7924	SC16		1.5	0.7881
S17		1.5	0.7829	SC17		1	0.7673
S18		1	0.7593	SC18	380	1	0.7346
				SC19		1.5	0.7571
				SC20		2	0.7775
				SC21	390	2	0.7534
				SC22		1.5	0.7373
				SC23		1	0.7214
				SC24	380	1	0.7431
				SC25		1.5	0.7603
				SC26		2	0.7774
				SC27	370	2	0.7989
				SC28		1.5	0.7931
				SC29		1	0.7602

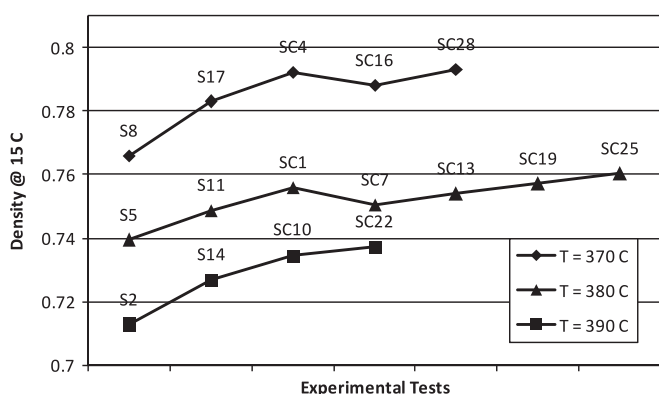


Fig. 3. Specific gravity of product samples for tests at LHSV = 1.5 h⁻¹ and different temperatures.

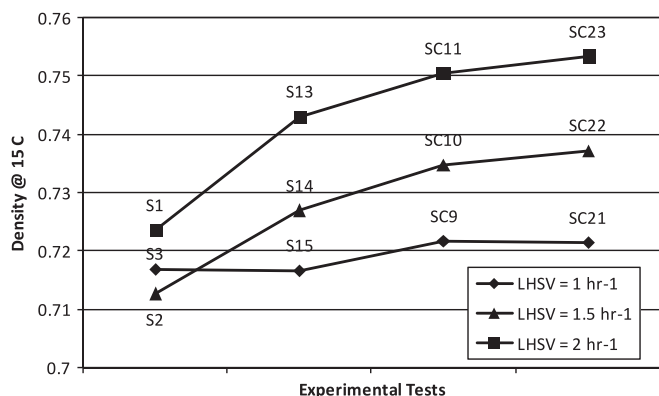


Fig. 4. Specific gravity of product samples for tests at T_{bed} = 390°C and different space velocities.

weight fraction of the distilled mixture. T_0 is the initial boiling point (T at $x = 0$), which can be obtained from the experimental distillation curve. A and B are two parameters to be determined from available experimental data through regression. Eq. (2) does not give a finite value for T at $x = 1$ (end point at 100% distilled). According to this model the final boiling point is infinite (∞) which is true for heavy residues. Theoretically, even for light products with a limited boiling range there is a very small amount of heavy compound since all compounds in a mixture cannot be completely separated by distillation. For this reason predicted values from Eq. (2) are reliable up to $x = 0.99$, but not at the end point.

The main application of Eq. (2) is to predict complete distillation curve from available experimental data. It can be applied for any type of distillation data, ASTM D-86, ASTM D-2887 (simulated distillation), TBP (true boiling point), EFV (equilibrium flash vaporization) and ASTM D-1160 as well as TBP at reduced pressures or EFV at elevated pressures. In the case of simulated distillation (SD) curve data, x is cumulative weight fraction distilled. Eq. (2) is also perfectly applicable to molecular weight, density (or specific gravity) and refractive index distribution along a distillation curve for a petroleum fraction and crude oils.

Eq. (2) can be converted into the following linear form:

$$Y = C_1 + C_2 X \tag{3}$$

where

$$Y = \ln \left[\frac{T - T_0}{T} \right] \quad \text{and} \quad X = \ln \left(\ln \left[\frac{1}{1-x} \right] \right) \tag{4}$$

In this case, constants C_1 and C_2 can be determined using linear regression of Y versus X , with an initial guess for T_0 . The parameters A and B are then determined from C_1 and C_2 as:

$$B = \frac{1}{C_2} \quad \text{and} \quad A = B e^{C_1 B} \tag{5}$$

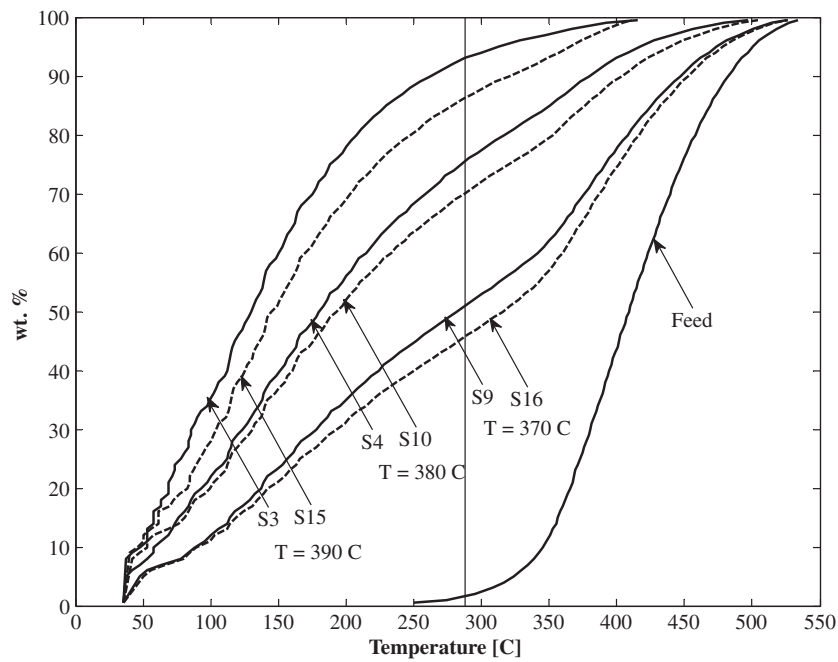


Fig. 5. Boiling point curves for sample tests at LHSV = 2.0 h⁻¹ and different bed temperatures.

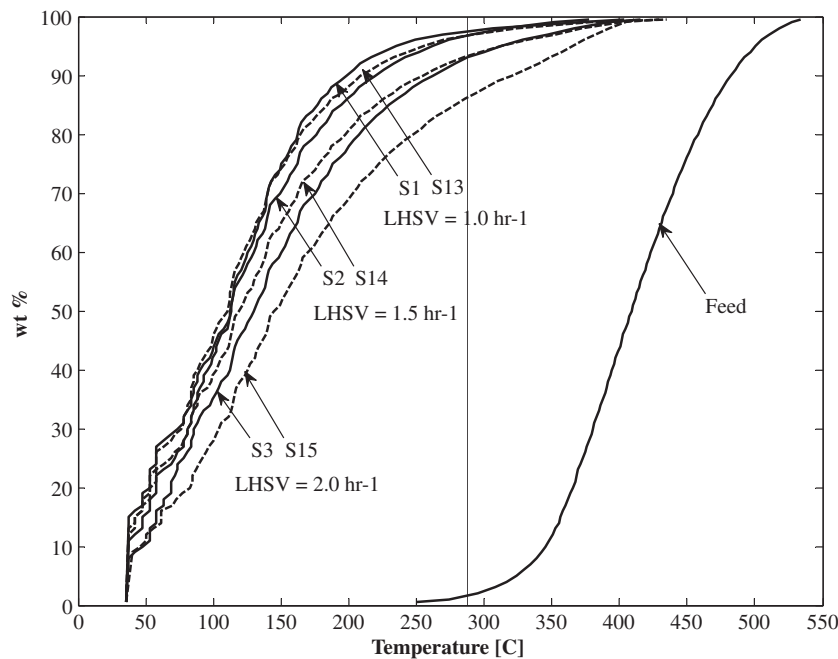


Fig. 6. Boiling point curves for sample tests at $T_{bed} = 390\text{ }^{\circ}\text{C}$ and different space velocities.

For fractions with very high and uncertain final boiling point, such as atmospheric or vacuum residues and heptane-plus fraction of crude oils, the value of B can be set as 1.5 [12]. However, for various petroleum fractions with finite boiling range, the parameter B should be determined from the regression analysis. The value of B for light fractions is higher than that of heavier fractions and is normally greater than 1.5.

The property that will be used in this study is the specific gravity, which can be easily measured, online or offline. The specific gravity (SG) will be related to the boiling point data by correlating

the parameters A , B and T_0 to the experimental SG values of the product samples. As described below, cubic equations were mainly used in developing the correlations.

Parameter estimation was performed using the SOLVER add-in tool in MS Excel. The objective function used in both linear and nonlinear regressions is the root mean squares error (RMSE) defined as:

$$RMSE = \left[\frac{1}{N} \sum_{i=1}^N (T_i^{calc} - T_i^{exp})^2 \right]^{1/2} \quad (6)$$

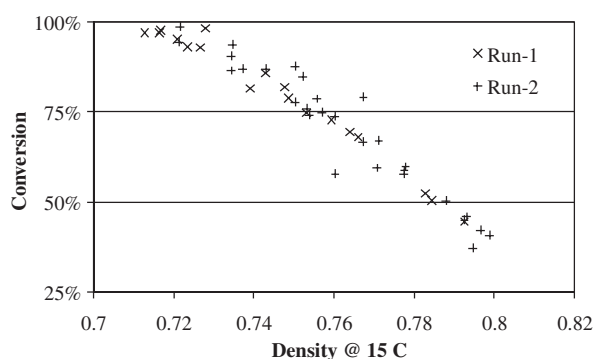


Fig. 7. Relationship between conversion and density of the cracked product samples.

where N is the total number of data points used in the regression and T_i^{calc} is the boiling point temperature of fraction i evaluated by Eq. (2). The goodness of the estimated parameters can be quantified by maximizing the coefficient of correlation (R^2) defined as:

$$R^2 = 1 - \frac{S_{total}}{S_{error}} \quad (7)$$

where, S_{total} is the total sum of squares (proportional to the sample variance) and S_{error} is the sum of squared errors defined as:

$$S_{total} = \sum_{i=1}^N (T_i^{exp} - \overline{T^{exp}})^2$$

$$S_{error} = \sum_{i=1}^N (T_i^{calc} - T_i^{exp})^2 \quad (8)$$

where $\overline{T^{exp}}$ is the mean value of the experimental data used in the regression. Another measure that will be used in evaluating the developed model is the average absolute deviation error (AAD) defined as:

$$AAD = \frac{1}{N} \sum_{i=1}^N \left| 1 - \frac{T_i^{calc}}{T_i^{exp}} \right| \quad (9)$$

4. Model prediction and validation

The parameters T_0 , A , and B in Eq. (2) were estimated using the 18 samples of Run-1 (S1–S18), while Run-2 samples (SC1–SC29) were used in model validation. More than 95 data points were used for each sample covering the boiling points range from 0.5 to 99.5 wt.% distilled. Three different methods were used in parameter estimation, these are:

1. The value of B was fixed as 1.5, and nonlinear regression was used to estimate T_0 and A .
2. Nonlinear regression was used to estimate the value of T_0 , while A and B were determined by linear regression and using Eq. (3)–(5).
3. Nonlinear regression was used to estimate the three parameters, T_0 , A and B .

The average %AAD errors resulted from using the three methods were 1.542 ± 0.847 , 1.736 ± 1.127 and 1.832 ± 1.279 , respectively, while the corresponding R^2 values were 0.988 ± 0.011 , 0.977 ± 0.036 and 0.983 ± 0.021 . Hence, fixing the value of B as 1.5 gives the best estimates. The main deficiency of the other two methods was in estimating the value of the initial boiling point. They generally gave low T_0 values, and for those samples with reasonable T_0 estimates, the values of B were close to 1.5. Moreover, since the samples studied are heavy fractions (VGO),

then fixing the value of B complies with the recommendation given by Riazi [12].

Values of the estimated parameters are listed in Table 2 for all samples of Run-1 with their corresponding %AAD and R^2 values. The table shows that the errors are generally within 1.0–1.5% except for few samples. Parameters A and T_0 given in Table 2 were correlated to the SG values of the 18 product samples using the following cubic equations:

$$A = a_1 + b_1 SG + c_1 SG^2 + d_1 SG^3$$

$$T_0 = a_2 + b_2 SG + c_2 SG^2 + d_2 SG^3 \quad (10)$$

The resulted values of the coefficients are given in Table 3. They reproduce the constants T_0 and A with %AAD of 2.5 and 9%, respectively.

The developed prediction model consists of the distribution function given by Eq. (2) and the correlations given by Eq. (10). Given the SG of the cracked product, the values of T_0 and A are first evaluated using Eq. (10), followed by estimating the entire boiling point range using Eq. (2). The proposed model was validated using the experimental product samples for both Runs-1 and Run-2. Deviation errors (%AAD) and coefficients of correlation (R^2) for all product samples are listed in Table 4. Note that experimental data for Run-1 were used in estimating the parameters of the model, while those of Run-2 may be considered as blind data because they were obtained independently in another set of experimental runs.

Table 4 shows that the proposed model succeeded in predicting the distillation data with acceptable accuracy. The average deviations for Run-1 and Run-2 are 2.679% and 4.485%, respectively, and the average R^2 values are 0.949 and 0.898, respectively. Most deviations were found at the initial (less than 5%) and final (more than 95%) parts of the distillation curves. If these portions are excluded from the calculation of the errors, then the %AAD will be reduced to around 2% for Run-1 and 3% for Run-2.

Table 2
Values of the estimated parameters using samples of Run-1.

Sample #	SG	T_0 /K	A	B	%AAD	R^2
S1	0.7169	292.4	0.3448	1.5	1.5	0.976
S2	0.7127	278.9	0.4627	1.5	1.1	0.995
S3	0.7236	288.6	0.5208	1.5	0.5	0.997
S4	0.7532	288.0	0.9279	1.5	1.1	0.990
S5	0.7393	275.0	0.9262	1.5	1.2	0.981
S6	0.7211	262.3	0.6299	1.5	1.3	0.990
S7	0.7480	268.4	0.9887	1.5	1.2	0.994
S8	0.7659	282.8	1.1458	1.5	1.7	0.995
S9	0.7845	304.5	1.2911	1.5	3.7	0.974
S10	0.7641	282.8	1.1047	1.5	1.6	0.996
S11	0.7488	276.2	0.9700	1.5	1.1	0.995
S12	0.7281	299.4	0.3900	1.5	1.46	0.985
S13	0.7167	282.8	0.4118	1.5	1.0	0.992
S14	0.7269	276.7	0.5683	1.5	1.0	0.994
S15	0.7431	287.4	0.6725	1.5	1.0	0.996
S16	0.7924	307.5	1.2040	1.5	3.1	0.952
S17	0.7829	313.0	1.1268	1.5	3.0	0.984
S18	0.7593	289.8	0.9599	1.5	1.2	0.996

SG is the specific gravity at 15.5 °C.

Table 3
Coefficients for correlating the values of the parameters T_0 and A Eq. (10).

Coefficients	T_0	A
A	−36324.2	1308.43
B	153860.32	−5325.07
C	−215301.3	7206.21
D	100306.17	−3240.76

Table 4
Validation of the prediction model for the product samples of Run-1 and Run-2.

Run-1			Run-2		
Sample	%AAD	R^2	Sample	%AAD	R^2
S1	2.333	0.957	SC1	3.404	0.947
S2	1.668	0.989	SC2	4.147	0.921
S3	2.627	0.982	SC3	9.882	0.728
S4	2.128	0.986	SC4	6.995	0.821
S5	3.615	0.940	SC5	2.830	0.924
S6	1.434	0.987	SC6	1.538	0.987
S7	1.874	0.986	SC7	1.969	0.985
S8	1.865	0.965	SC8	7.083	0.804
S9	5.731	0.865	SC9	6.128	0.791
S10	1.763	0.964	SC10	4.877	0.846
S11	1.360	0.990	SC11	4.395	0.735
S12	3.635	0.843	SC12	5.024	0.871
S13	1.445	0.982	SC13	1.646	0.988
S14	1.414	0.991	SC14	3.433	0.955
S15	2.013	0.971	SC15	7.231	0.866
S16	6.592	0.822	SC16	5.613	0.886
S17	5.104	0.883	SC17	3.178	0.877
S18	1.619	0.972	SC18	1.805	0.989
Average	2.679	0.949	SC19	2.959	0.957
Minimum	6.592	0.991	SC20	4.658	0.905
Maximum	1.360	0.822	SC21	3.035	0.975
			SC22	2.317	0.989
			SC23	2.243	0.986
			SC24	4.077	0.946
			SC25	2.896	0.956
			SC26	3.794	0.923
			SC27	7.736	0.806
			SC28	6.454	0.837
			SC29	8.563	0.836
			Average	4.485	0.898
			Minimum	9.882	0.989
			Maximum	1.538	0.728

Fig. 8 compares the experimental and predicted distillation data for three samples from Run-1. They correspond to samples with average (S3), minimum (S11) and maximum (S16) %AAD prediction errors (Table 4). It is clear from the plots that sample S16 has the maximum deviation due to the differences in the concavi-

ties of the distillation curves. The distribution function given by Eq. (2) describes the distillation data as an s-shape curve. Prediction results showed that the errors increased as the shape of the distillation curves deviates from the s-shape. Examples for such deviations are shown in Figs. 8–10 for samples S16, SC20 and SC22, respectively. Hence, the shape of the distillation curve contributes directly to the accuracy of the predictions.

Effects of space velocity and operating temperature on the prediction accuracy of the distillation data are shown in Figs. 9 and 10, respectively. The plots show clearly that maximum deviations are observed at $LHSV = 2 \text{ h}^{-1}$ and $T = 370 \text{ }^\circ\text{C}$, which correspond to the lowest operating severity. Hence, the accuracy of the proposed model increases with increasing operating severity, which corresponds to increasing cracking yield.

Another important parameter that will be used in assessing the prediction performance of the proposed model is the cracking conversion, which is calculated using Eq. (1). Values of the experimental and predicted conversion, for all product samples in Run-1 and Run-2, are compared using the parity plot shown in Fig. 11. The plot clearly indicates wide deviations below 60% conversion, and excellent agreement at high conversions. These results support the conclusion that the prediction model is more accurate at higher reaction severities. Deviations in predicting the cracking conversions can be clearly observed in Figs. 8–10 in which the vertical dotted line indicates the $288 \text{ }^\circ\text{C}$ border temperature.

Obviously errors involved with the measurements have contributed to the deviations observed in these figures. But for majority of sample predicted distillation curves agree well with measured values and are within experimental uncertainty.

5. Conclusions

In this paper a series of tests were conducted on hydrocracking of vacuum gas oil under different operating reactor conditions. A predictive model has been proposed to predict the entire distillation curve and the cracking conversion from the knowledge of the specific gravity of the cracked product. The model parameters were estimated using one set of experimental

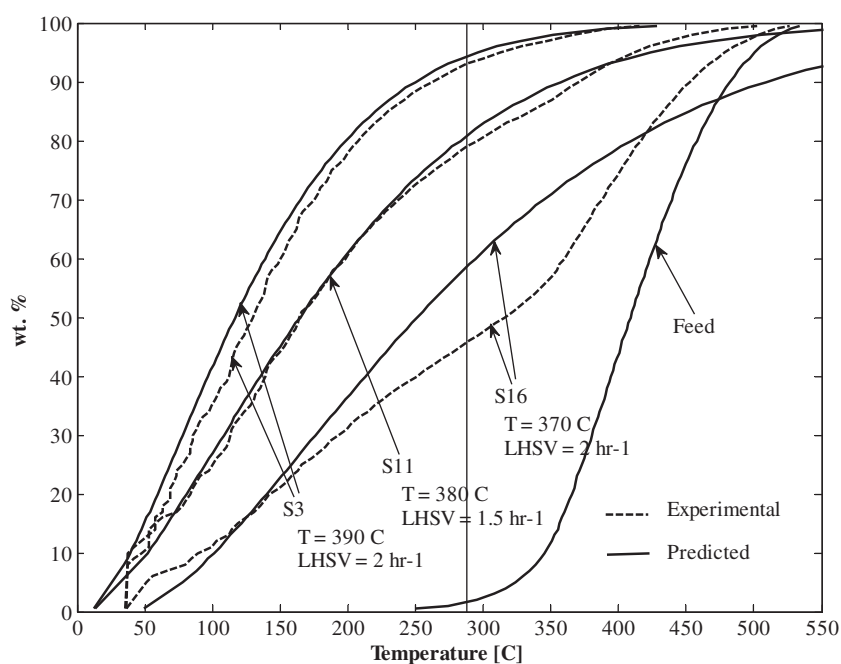


Fig. 8. Comparing experimental and predicted distillation data for three samples from Run-1.

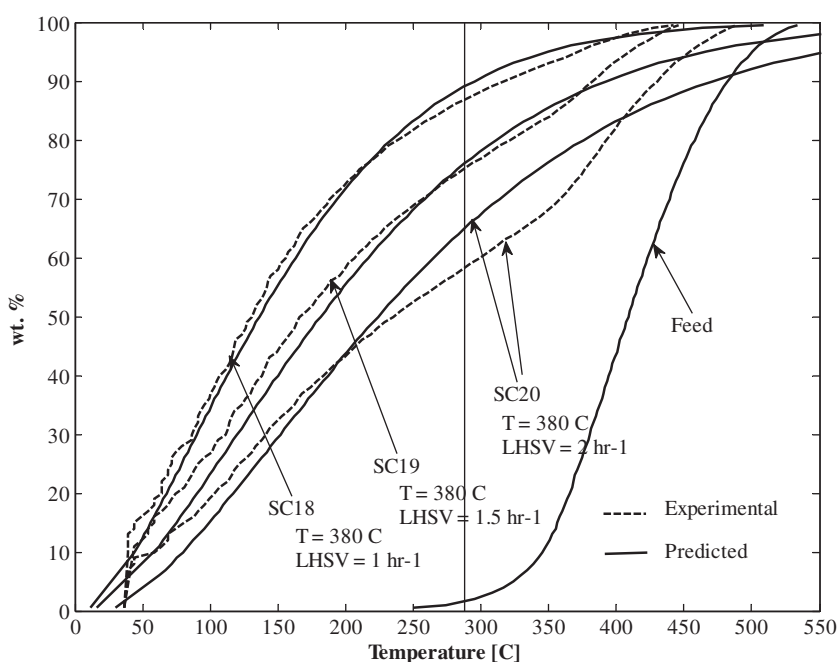


Fig. 9. Effect of LHSV on predicting the distillation data for three samples from Run-2.

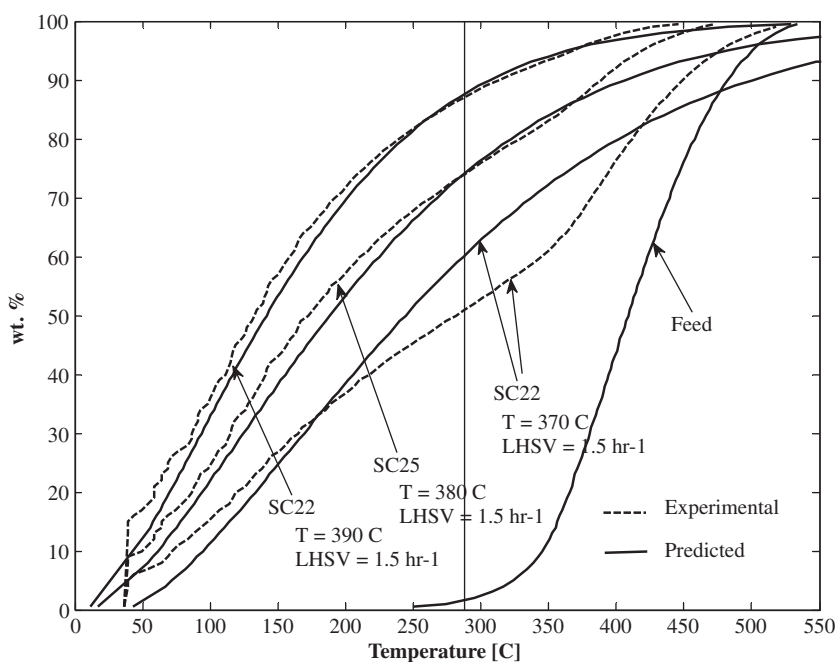


Fig. 10. Effect of temperature on predicting the distillation data for three samples from Run-2.

runs (Run-1), while the model was validated using another set of experimental runs (Run-2). The paper presented also the methodology that should be followed to estimate new values of the parameters in case the feedstock and/or the catalyst type are changed.

The predictions of the proposed model showed very good agreement with the experimental results. They are exceptionally accurate at high operating severities (high reaction temperatures and low space velocities), and may be considered acceptable at low

severities. Deviations are mainly attributed to the fact that the distribution model used in this study was a two-parameter model for simplicity in predictions.

Considering the fact that the specific gravity of the samples is the only required measurement, the proposed model may be considered suitable for the development of an online soft sensor to estimate the conversion as well as the product distribution of hydrocracking units in refineries. Moreover, such soft-sensor can play a significant role in improving the control strategy of the fractionators that follow the

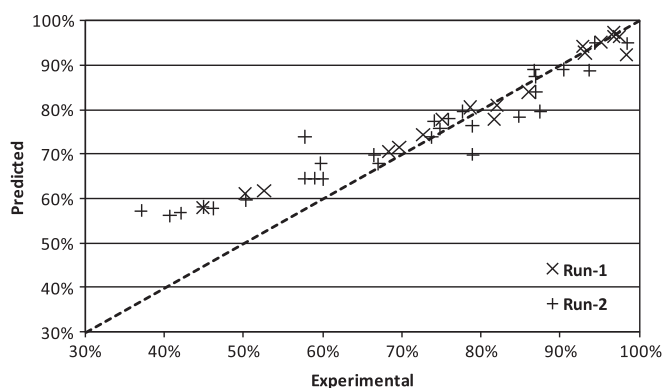


Fig. 11. Comparing experimental and predicted cracking conversion.

reaction section of the process. The benefits include better product yield, effective energy utilization, and consistent product quality.

Acknowledgements

The experimental work was financially supported by Kuwait Foundation for the Advancement of Sciences (KFAS). The authors acknowledge also the technical support provided by the pilot-plant personnel at KISR Petroleum Research and Studies Center (PRSC).

References

- [1] Meyers RA. Handbook of petroleum refining processes Part 7. 3rd ed. New York: McGraw-Hill; 2004.
- [2] Scherzer J, Gruia AJ. Hydrocracking science and technology. New York: Marcel Dekker; 1996.
- [3] Alhumaidan F. Modeling Hydrocracking kinetics of atmospheric residue by discrete and continuous lumping. MSc Thesis, College of Graduate Studies, Kuwait University; 2004.
- [4] Corma A, Martinez A, Martinezsoria V, Monton JB. Hydrocracking of vacuum gasoil on the novel mesoporous MCM-41 aluminosilicate catalyst. *J Catal* 1995;153(1):25–31.
- [5] Valavarasu G, Bhaskar M, Balaraman KS. Mild hydrocracking—a review of the process, catalysts, reactions, kinetics, and advantages. *Petroleum Science and Technology* 2003;21(7/8):1185–205.
- [6] Kadlec P, Gabrys B, Strandt S. Data-driven soft sensors in the process industry. *Computers and Chemical Engineering* 2009;33:795–814.
- [7] Lababidi HMS, Shaban HI, Al-Radwan S, Alper E. Simulation of an atmospheric desulfurization unit by quasi-steady state modeling. *Chemical Engineering & Technology* 1998;21:193–200.
- [8] Jos de Assis A, Maciel Filho R. Soft sensors development for on-line bioreactor state estimation. *Computers and Chemical Engineering* 2000;24(2):1099–103.
- [9] Lukec ISertić-Bionda K, Lukec D. Prediction of sulphur content in the industrial hydrotreatment process. *Fuel Processing Technology* 2008;89:292–300.
- [10] Lababidi HMS, Baker CGJ. Fuzzy modeling – An alternative approach to the simulation of dryers. In: Proc. 15th International drying symposium (IDS 2006), Vol. A, Budapest, Hungary, 20–23 August, 2006. p. 258–264.
- [11] Whitson CH, Anderson TF, Soreide I. Application of the gamma distribution model to molecular weight and boiling point data for petroleum fractions. *Chemical Engineering Communications* 1990;96:259–78.
- [12] Riazi MR. Distribution model for properties of hydrocarbon-plus fractions. *Industrial and Engineering Chemistry Research* 1989;28:1731–5.
- [13] Riazi MR. A continuous model for c7+ characterization of petroleum fractions. *Industrial and Engineering Chemistry Research* 1997;36:4299–307.
- [14] Riazi MR. Characterization and properties of petroleum fractions. Conshohocken, PA: ASTM International; 2005.